JOURNAL OF MATERIALS SCIENCE 32 (1997) 5761–5774

Sizing related kinetic and flow considerations in the resin infusion of composites

V. M. KARBHARI
Department of Applied Mechanics and Engineering Sciences, Mail Code 0085, University of California, San Diego, La Jolla, CA 92093-0085, USA

G. R. PALMESE
Centre for Composite Materials, University of Delaware, Newark, DE 19716, USA

Fibres used in preforms of resin transfer moulded (RTM) composites are coated with sizings, binders, and/or finishes that serve multiple purposes, including facilitating handling, protection of the fibres from compaction and process induced damage (including notching), aiding in compatibility and wetting of the fibres by the resin, and overall enhancement of the behavioural response of the composites. In this investigation four different sizings applied to S2 glass fibres are shown to significantly affect two aspects of RTM processing – resin infusion, and cure. In both cases phenomena at the microscopic level are seen to affect response variables at the macroscopic level. On a microscopic level, the behaviour of a thermosetting resin based composite is affected by the formation of interphase regions that greatly affect the cure kinetics and hence the mechanical and physical properties of the composite, which are dependent on the inter-constituent variations in local properties such as modulus and glass transition temperature. Similarly fibre–sizing–resin interactions occurring during the infusion stage affect wet-out and local flow behaviour through the development of stoichiometric imbalances in local regions. It is shown that the molecular interactions between the constituents (as initiated by the sizing) are affected by processing conditions such as temperature and rate of resin flow, and that heat evolution and resin rheology may be affected by the stoichiometric imbalances resulting from interphasial level reactions.

1. Introduction

In recent years, enhanced processing options such as resin transfer moulding (RTM), and resin infusion type processes in general, have lead to an increased amount of attention being paid to thermosetting resin based composites by the automotive and aerospace industries. The processing of such materials may appear to be simple, but is in fact, complex, since it requires a good understanding and control of both resin system rheology and the kinetics of polymerization reactions in the presence of the fibrous reinforcement. The aspects of interdependence and criticality of the materials selection and processing stages are of special significance in composite processes such as resin infusion wherein the two stages of fibre preforming and resin injection are distinct in phase, but coupled in materials selection and processing related aspects. In the first phase of the process (i.e., fibre preforming), the fibres are arranged and combined to meet the microstructural and geometric requirements of the part. The preform is then placed into the mould and the mould is closed (Fig. 1). The second phase of the process (i.e., resin injection and cure) involves the transfer of resin from holding tanks into the preform. During this infusion stage, the resin "wets-out" the reinforcement and undergoes polymerization. Once the composite develops sufficient dimensional stability, it may be removed from the tool and post-cured (as appropriate). It should be noted that although the preform architecture is defined in the first stage of the process, reorientation of the fibres is possible (and, in fact, often occurs) which could lead to serious design deficiencies if aspects such as fibre volume fraction and tool design are not addressed appropriately in this loop. An error in the former can lead to significant fibre wash, whereas one in the latter can lead to movement of preform elements and the development of resin-rich areas. Added to these aspects are those related to the issue of scale between flow at the bundle level and that at the fibre level, and that of cure in the composite as compared to that adjacent to a fibre in the neat resin.

Most fibres used in composites are coated with sizings, binders, and/or finishes that serve multiple purposes, including facilitating handling, protection of the fibres from compaction and process induced damage (including notching), aiding in compatibility and wetting of the fibres by the resin, and overall enhancement of the behavioural response of the composites. Examples of sizing materials include epoxies, starches,

0022–2461

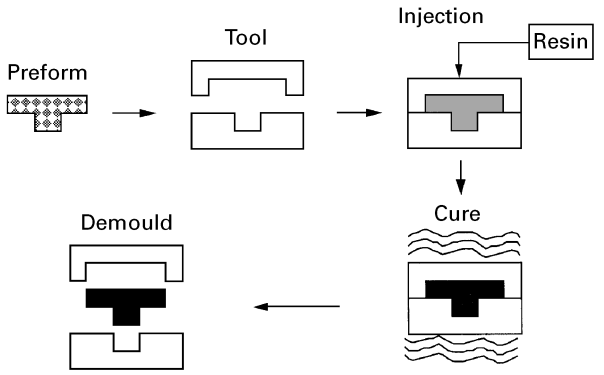

Figure 1 Schematic of the resin transfer moulding process.

silanes, and chrome complexes which to varying degrees also serve as coupling agents. These agents chemically and physically modify fibre surfaces enabling enhanced bonding of the fibre surfaces with the matrix during cure. In order to tailor surface characteristics, commercial fibre sizings are optimized in thickness and composition for specific resin types, with thickness generally extending to about 0.15 μm for glass and carbon fibres. The reaction products formed through chemical interactions between the sizing and the resin may alter the nature of the polymeric resin material in the vicinity of the fibre surface. This region is generally known as the interphase with properties that can be different from those of both the fibre and the bulk resin. Indeed under appropriate conditions sizings have been shown to cause the formation of interphase regions which possess gradients in material properties and affect composite behaviour [1, 2].

Sizings can affect two aspects of composite performance: composite behavioural characteristics and processing performance. In both cases phenomena at the microscopic level are seen to affect response variables at the macroscopic level. On a microscopic level, the behaviour of a thermosetting resin based composite is affected by the formation of interphase regions that greatly affect the cure kinetics and hence the mechanical and physical properties of the composite, which are dependent on the inter-constituent variations in local properties such as modulus and glass transition temperature. Similarly fibre–sizing–resin interactions occurring during the infusion stage affect wet-out and local flow behaviour through the development of stoichiometric imbalances in local regions. These imbalances may in turn influence performance by affecting apparent cure kinetics causing local gelation and hot-spots, as well as macroscopic flow behaviour through local rheological effects (changes in viscosity due to increased concentration of sizings, etc.). It is important to note that the thermal and rheological effects due to the presence (or absence) of sizings are not separable in RTM systems since they are coupled at the microscopic level. For example, the molecular interactions between the constituents (as initiated by the sizing) are affected by processing conditions such as temperature and rate of resin flow. On the other hand, heat evolution and resin rheology may be affected by the stoichiometric imbalances resulting from interphasial level reactions. It is thus critical that due importance be given to the role of sizings not just in terms of the final compatibility between the fibre and matrix as related to bonding, but also in terms of effects on processing itself. In this paper we focus on aspects related to the effects of sizing on flow and cure during the infusion of a vinylester resin system through a S2 glass preform with the intention of developing an understanding of the microlevel phenomena that affect macroscopic behavioural response of an RTM composite.

2. Materials and materials characterization

Although the aspects of resin flow and cure are highly coupled in resin infusion processes, the current investigation looked at each individually, so as to focus on the microscale phenomena in both cases. In addition to the studies aimed at flow and cure, surface characterization was conducted using Fourier transform infrared spectroscopy (FTIR), and dynamic contact angle (DCA) measurements for the determination of contact angles. S-2 glass rovings provided by Owens Corning with sizings designated as 365, 933, 449 and 463 were used in this investigation. Details related to the rovings are given in Table I. It should be noted that the 933 sizing system was designed for compatibility with higher temperature cure resin systems such as BMI and PEEK, the 365 system was designed for use with vinylesters and polyesters, whereas the 449 and 463 sizing systems were designed for use with epoxies. Since the actual composition of sizings is a closely guarded secret in industry, an attempt was made to gain some insight into the differences in sizing composition among the four sizings used in this investigation by stripping the fibres with acetone and analysing the dissolved materials using transmission FTIR. The FTIR spectra of the stripped material are shown in Fig. 2, together with the spectra from Epon-828. It can be seen that although the 463, 449 and 365 fibres show similar peaks at 1120, 1080, 940 and 3400 cm^{-1}, the 933 spectrum displays only the 1120 cm^{-1} peak. The 1120 cm^{-1} absorption peak can be associated with silane-derived silicon species, which interestingly enough is common to all four types of fibres. Both the 1120 cm^{-1} and the 1080 cm^{-1} peaks can be associated with the Si–O–Si asymmetric stretch [3–5] and the Si–O–C asymmetric stretch [3]. The absorption peaks at 940 and 3400 cm^{-1} correspond to the Si–OH stretch [3–5]. Based on the lack of Si–O–C

TABLE I Details of roving types investigated

Sizing type	Resin compatability	Filament diameter (μm)	Number of filaments in a roving
365	Vinylester, polyester	13	2000
933	High temperature resins (PEEK, BMI)	9	4200
449	Epoxy	9	4200
463	Epoxy	9	4200

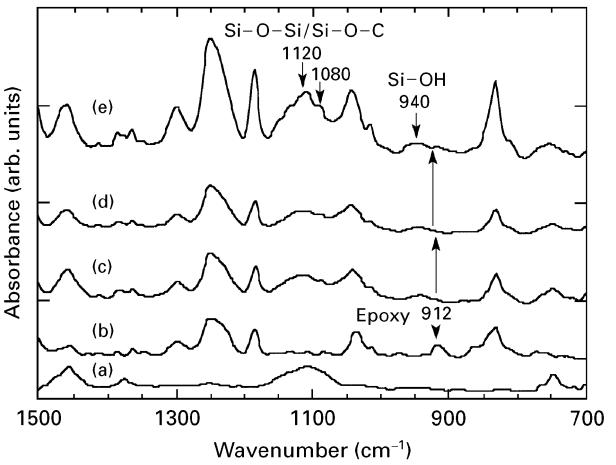

Figure 2 FTIR spectra of sizing material stripped from S2 glass fibres using acetone. Key: (a) 933; (b) EPON-828; (c) 365; (d) 449 and (e) 463 sized fibres.

type peaks in the 933 spectra, it is hypothesized that although all four sizings show the presence of silane derived silicon, the 933 contains more fully condensed silane whereas the 463, 449 and 356 fibre sizings contain some hydrolysed material. Moreover it is clear from a comparison of the sizing spectra with that obtained from FTIR spectra of Epon 828 that the 463, 449 and 365 sizings contain a substantial amount of unbound epoxy, which is absent in the spectrum for 933.

The resin system used in the present investigation was a Dow Derakane 411-C50 vinylester. The system has a 50 vol % styrene content and a heat distortion temperature of 210–220 °F. When tested with a Brookfield LVT-DV1 digital viscometer at room temperature over a range of shear rates from 1 to 20 s^{-1}, the resin was seen to display Newtonian behaviour with a viscosity of 135 centipoise (cps). The resin has a nominal tensile strength and modulus of 75–82 MPa and 3.4 GPa respectively. In order to characterize the surface tension of the resin system, a dynamic contact angle analyser, based on the micro-Wilhemy technique [6] was used for the determination of the polar and dispersive components and the total surface free energy. Glass slides and Teflon® (PTFE) samples were immersed at a rate of 75 μm min^{-1} into the fluid. The surface tension, γ_{IV}, of the resin system was determined using the glass slide since the high energy surface provides a zero contact angle. The dispersive component was determined using Teflon, which is a highly dispersive solid (18.10 dynes cm^{-1} dispersive and 0.93 dynes cm^{-1} polar). Following Kaeble [7], a manipulated form of the Young–Dupré equation was used, such that

$$1 + \cos\theta = \frac{2(\gamma_{SV}^{D}\gamma_{IV}^{D})^{1/2}}{\gamma_{IV}} + \frac{2(\gamma_{SV}^{P} + \gamma_{IV}^{P})^{1/2}}{\gamma_{IV}} \quad (1)$$

where γ_{SV}, γ_{IV} and θ are the surface free energy between solid and vapour, surface free energy between liquid and vapour, and the equilibrium contact angle that the liquid forms with the solid, respectively. The superscripts, *D* and *P*, differentiate between the dispersive and polar components respectively. Based on "receding data" from the micro-Wilhemy tests the polar, dispersive and total surface free energies of the 411–C50 resin system were determined to be 1.2 ± 1.0, 34.2 ± 1.0 and 35.4 ± 0.7 dynes cm^{-1} respectively, depicting a strongly dispersive system.

TABLE II Components of surface free energies (dynes cm^{-1})

Material type	γ^{p}	γ^{d}	γ^{t}
S2 glass with 449 sizing	10.88 ± 2.51	44.44 ± 4.52	55.33 ± 5.17
S2 glass with 463 sizing	6.94 ± 1.40	45.07 ± 2.80	52.00 ± 3.13
S2 glass with 933 sizing	12.60 ± 3.02	32.50 ± 3.95	45.10 ± 4.97
S2 glass with 365 sizing	8.60 ± 1.18	33.09 ± 1.92	41.69 ± 2.25
411-C50 resin	1.2 ± 1.0	34.2 ± 1.0	35.4 ± 0.7

Polar and dispersive components of the surface energy for the differently sized fibres were obtained by measuring the contact angles of these fibres in a series of test fluids of known polar and dispersive surface tensions and analysing the results which are listed in Table II. The contact angles were obtained using the micro-Wilhemy technique. Fibres were cut and glued to a wire using a cyanoacrylate adhesive. Advancing contact angles were recorded at an immersion rate of 20 μm s^{-1}. Values of fibre radii obtained from the manufacturer's specifications were checked with values obtained using the DCA and octane as the wetting fluid.

3. Flow characterization

The infusion of resin into a fibrous preform is one of the most critical steps in resin transfer moulding. Complete impregnation of the preform is essential, although not sufficient, for the formation of a void free part. It should be noted that in RTM the fabric architecture creates a network of flow paths and channels through which the resin must flow in order to fill the tool. These flow channels exist between fibre bundles, and within them – between individual filaments, with diameters being several orders of magnitude smaller than the average total gap-width, causing the creation of additional stresses and resistance to flow due to factors such as fibre architecture, capillary flow and pressure, and surface tension effects. Traditionally flow through preforms has been treated as analogous to flow through porous media, describable by Darcy's law:

$$\bar{u} = -\frac{K}{\eta}\nabla P \quad (2)$$

which relates the superficial velocity of fluid flow, $\bar{u}$, to the pressure gradient, ∇P, through the ratio of permeability, *K*, to the fluid viscosity, η. Since most performs, even if treated as two-dimensional porous media are orthotropic, the pressure–flow relationship can be treated, after neglecting effects of velocity

profile through the thickness, in terms of gap-wise averaged velocities as:

$$\begin{pmatrix} \bar{u}_x \\ \bar{u}_y \end{pmatrix} = \frac{1}{\eta} \begin{bmatrix} K_{xx} K_{xy} \\ K_{xy} K_{yy} \end{bmatrix} \begin{pmatrix} 2P/2x \\ 2P/2y \end{pmatrix} \quad (3)$$

where $\bar{u}_x$ and $\bar{u}_y$ are the gap-wise averaged velocities in the x and y direction respectively, $2P/2x$ and $2P/2y$ are the pressure gradients in the appropriate directions, and K_{xx}, K_{yy} and K_{xy} ($= K_{yx}$) are the components of the second-order permeability tensor. At this level, all interactions between the infusing resin and the fibre (including wetting and surface tension effects) are grossly lumped into the permeability tensor which is experimentally determined, and has been found to be a function of preform architecture and loading [8–11], flow rate [12], and fibre–resin interactions at the surface-tension level [13]. However, current levels of modelling are based on an idealization of pore structure geometry, neglecting details of flow field behaviour in the interstices between fibres and or bundles. In order to link permeability to microstructure as related to fibre diameter and volume fraction a Hagen–Poiseuille type equation can be assumed to govern flow in channels in the preform following Kozeny [14] as:

$$v_a = \frac{1}{8} \frac{R^2}{\eta} \frac{\Delta P}{L} \quad (4)$$

where R is the radius of a straight capillary tube and v_a is the actual average capillary velocity. Effects of tortuousity can be included through the use of a tortuousity term, L_e/L, as defined by Carman [15], or through an artificial correction factor such as suggested by Bird *et al.* [16]. The superficial velocity $\bar{v}$ observed at the macroscopic scale can then be related to microscopic flow represented by the average capillary velocity, ν_a, through the porosity, ϕ, and the tortuousity as:

$$\bar{v} = v_a \phi \frac{L}{L_e} \quad (5)$$

leading to the generally used Kozeny–Carman equation for macroscopic permeability (that attempts to incorporate microlevel phenomena), K, as:

$$K = \frac{1}{k_0 (L_e/L)^2} \frac{R_f^2}{4} \frac{\phi^3}{(1+\phi)^2} \quad (6)$$

Here k_0 is a dimensionless shape factor and R_f is the fibre radius. Although a number of improvements to this model, such as the incorporation of parallel, series and network models, have been made in an attempt to more closely replicate flow through an actual medium, none provide any fundamental increase in understanding of capillary flow [17]. It should be noted that although the Kozeny–Carman equation (and its derivatives with a variety of corrections) holds reasonably well in modelling isotropic granular media, it seems to show gross discrepancies in modelling transverse flow along aligned fibre beds, such as would be seen in capillary induced flow through a bundle.

Two major concerns about the use of a generic capillary model relate to: (a) the concept of hydraulic radius relating capillary flow to the flow around the bed, and (b) flow across fibres at low porosity. The former derives from the fact that the hydraulic radius concept is based on the principle that the pressure drop necessary for the resin to infuse with a given flow rate depends only on the dimension of the wetted boundary which is true for turbulent flow where shear almost exclusively takes place at the boundary layer. It is however not valid for creeping flows seen in RTM since a velocity profile is present across the infusion gap. Cell or array models have been developed in an attempt to address these concerns [18–21]. Unfortunately, all these developments, while very important for the computational modelling of flow through preform structures, do not assist in the development of further understanding of the link between flow at the macroscopic and microscopic levels (Fig. 3a) which is essential for further development of a true processing science base. Macro-flow (i.e., the flow of resin around the fibre tows of a preform) is primarily responsible for distributing the resin through the mould cavity, whereas micro-flow (i.e., the flow of resin between the

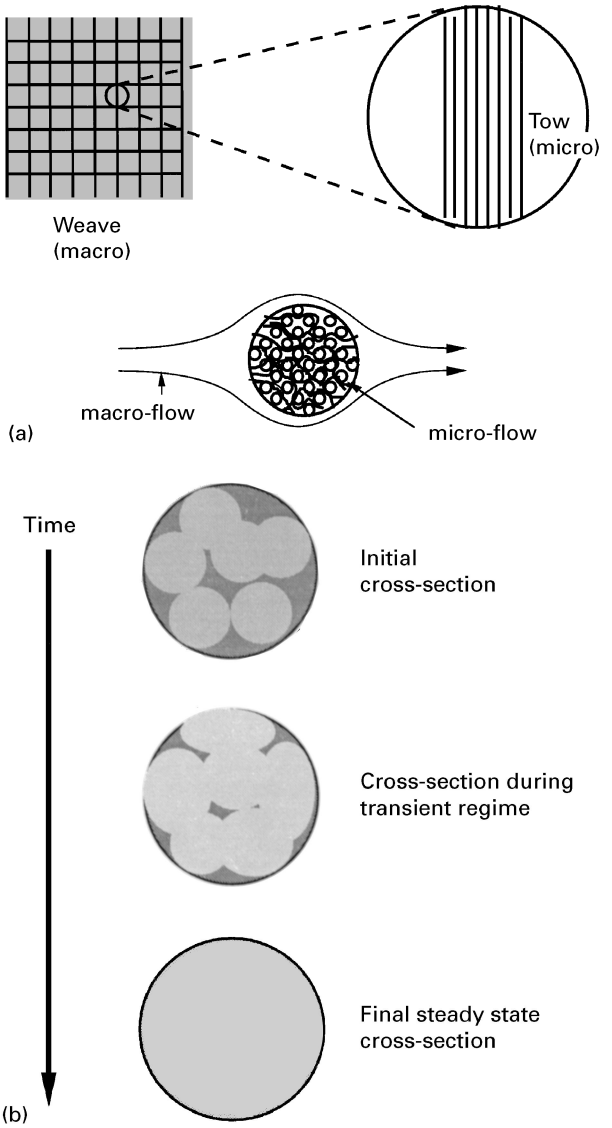

Figure 3 (a) Schematic showing difference between macro- and micro-flow and (b) schematic of resin infusion through fibre bundles as a function of time; key (■) areas open to flow between fibre tows and (□) areas open to flow between fibres in tows.

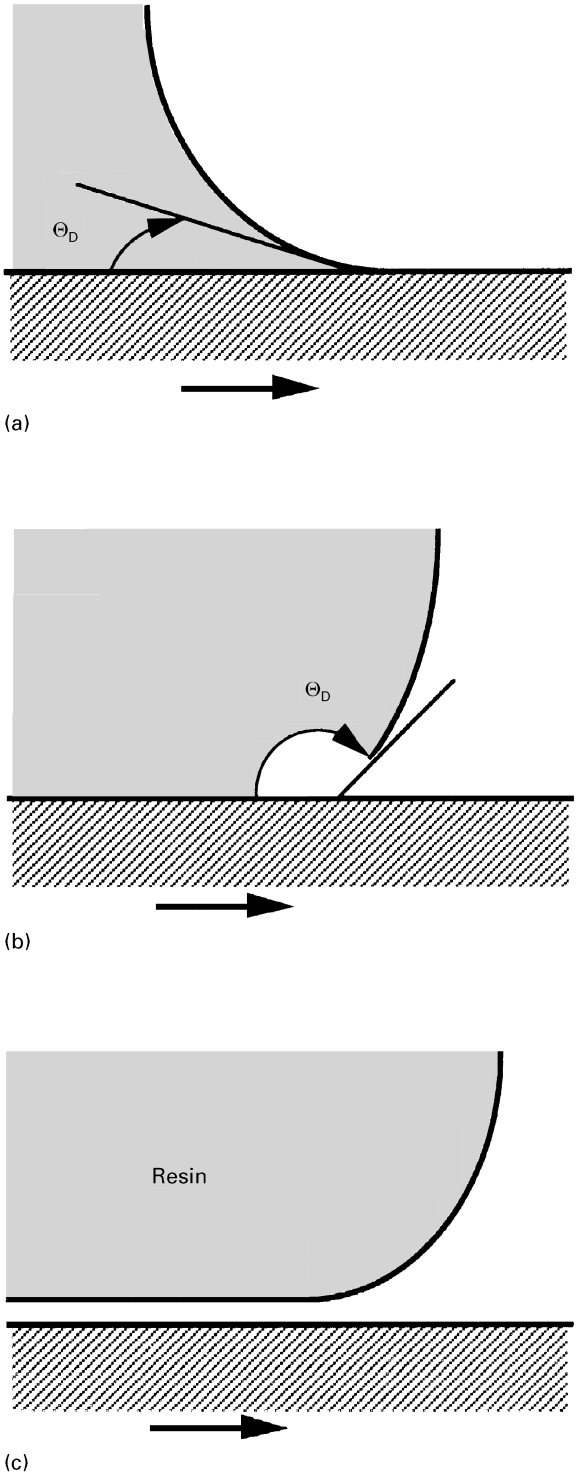

Figure 4 Schematic of effect of speed on contact angle and wettability; (a) low speed of resin flow; (b) intermediate speed of resin flow and (c) high speed of resin flow.

fibres in a fibre tow) is responsible for wetting the fibres within the fibre bundles. Recently attempts have been made to model the effect of tow permeability on the overall permeability of fibrous media [22, 23], and it was determined that tow permeability can lead to significant effects in velocity fields. As already shown by Palmese and Karbhari [24], the driving forces for micro-infusion, i.e., capillary pressures and pressure gradients between fibres, are highly affected by the presence of sizings and finishes.

Flow through a fibrous preform can generically be divided into two phenomena: (a) flow surrounding the fibre bundles, and (b) infiltration of resin into the tow as a result of capillary action and radial micro-flow. A schematic of this process at the level of a single tow is shown in Fig. 3b. Obviously phenomenon (a) is related to the macroscopic aspects of flow, whereas, phenomenon (b) is associated with micro-infusion. At the macroscopic level, it is well known that beyond a certain flow rate, the flow front can move in a way such that it traps air on the fibre surface causing voids in the final composite. Fig. 4(a–c) show schematics of the effect of rate of fluid flow on the wetting of a fibre surface. At low rates of infusion, the advancing dynamic contact angle is very similar to the static angle (Fig. 4a) which ensures complete wet-out. As the flow rate increases the dynamic contact angle rapidly increases (Fig. 4b) leading to the possibility of entrapped air in small pockets between the fibre surface and the moving resin flow front. At high enough flow rates the dynamic contact angle can approach 180° at which stage air is clearly entrained between the fibre surface and the advancing flow front (Fig. 4c). In RTM, a stage between Fig. 4(b and c) can easily be obtained with the wetting line showing serrations and unsteady profiles at high flow rates. However, beyond this knowledge, it is often assumed that provided that the resin and fibre surface are compatible, microscopic infusion of the bundle will occur on a similar time scale as that of mould filling. Since the driving forces for micro-infusion are capillary pressures, pressure gradients and surface interactions, the previous assumption is inherently flawed and the characteristic time for micro-infusion is actually substantially longer than the characteristic time required for macro-infusion. Failure to take this into account leads to the formation of a composite that appears to be fully impregnated at the macroscopic scale, yet has incomplete wetout and infusion within fibre tows. The development of an understanding of the driving forces of microinfusion is thus considered to be intrinsic to the complete development of a processing science base necessary for achieving high quality and repeatable RTM parts.

3.1. Experimental procedure

Due to continuously increasing cure of a resin system once catalysed, flow and infusion are usually accompanied by changes in viscosity of the resin. In order to isolate and experimentally evaluate flow at the micro-level uncatalysed resin was used in each case. The apparatus used in the flow experiments is shown in Fig. 5. Resin is injected at room temperature through a stainless steel tube (15 cm long and 0.38 cm ID) containing axially oriented fibre tows, using a two-stage pressure regulation system capable of controlling injection pressures to within 0.02 kPa. Outflow of resin was measured as a function of time to enable the evaluation of micro-infusion. A typical flow trace for such an experiment is shown in Fig. 6, depicting two distinct regimes: (a) a transient regime characterized by an initial rapid flow rate, and (b) a steady state regime possessing a significantly lower flow rate.

As discussed by Palmese and Karbhari [24] the duration of the transient period is an indication of the efficacy of resin-sizing interactions in promoting micro-infusion of the bundles. Stronger interactions lead to higher capillary pressures, allowing for more rapid intra-bundle infiltration. Fibre loadings and injection pressures were chosen for the experiments to allow the transient region to be recorded, and are listed in Table III. It should be remembered that all the rovings had 9 μm diameter fibres (~4200 filaments per roving) except for the roving set with fibres coated with the 365 sizing where the rovings were comprised of 13 μm diameter filaments (~2000 fiaments per roving).

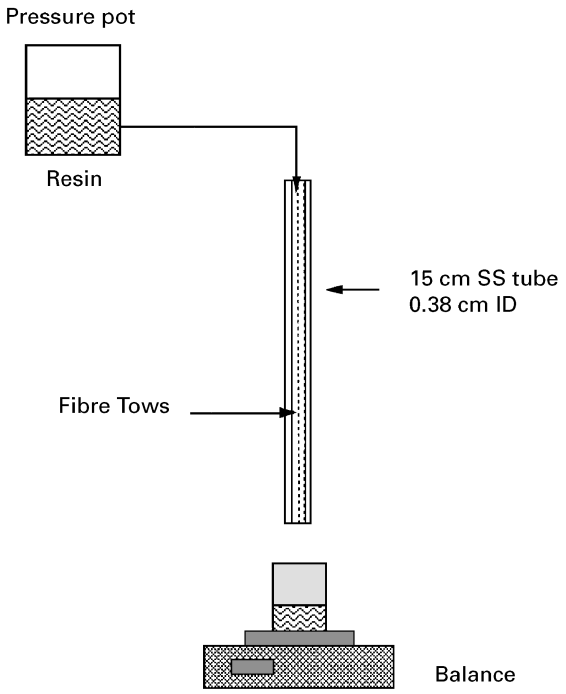

Figure 5 Schematic of the experimental setup for micro-infusion investigations.

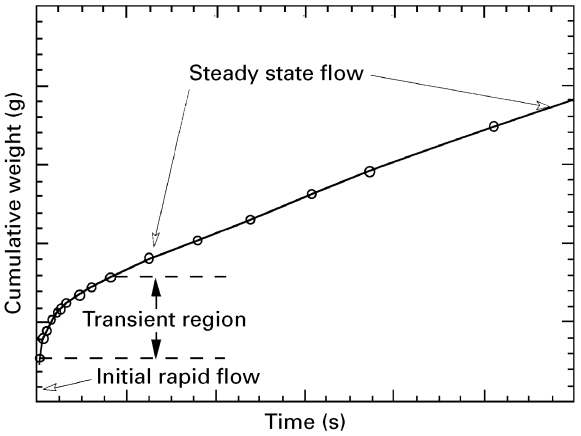

Figure 6 Typical flow trace showing the regimes of flow as a function of time.

3.2. Results and discussion

The effect of sizing type on overall flow behaviour is shown in Fig. 7, which depicts cumulative flow traces in terms of the total mass of resin flowing through the flow length as a function of time. In each of the curves the two main regimes are clearly seen characterizing the overall behaviour as resulting from two flow regimes. While all the cumulative flow traces exhibit a similar characteristic shape, sizing is seen to have a significant effect on flow behaviour, with the most significant changes being in the 365 sized system. Flow is initially rapid as the infusing resin follows the initial path of least resistance, through clear voids between fibres. During the ensuing transient period, the flow rate is attenuated until it reaches the significantly lower steady state value. The large changes in flow rate between the initial and steady state regimes can be seen from Table IV. The 933 sized system is seen to have the highest flow rate in the initial regime, whereas the 365 sized system shows the highest rate in the steady state regime. Based on visual observation, it is hypothesized that radial flow into the fibre tows induced by capillary action is the main driver for the change in regime. Infiltration of resin into fibre bundles spreads the fibres apart, thereby decreasing the macroscopic channelling volumes. The infusion of resin into the bundles spreads and evens the distribution of fibre bundles, decreasing macroscopic channelling volumes. Although the overall volume utilized for flow increases during this period, the ratio of surface area to volume also increases, causing a drastic decrease in flow rate through the system. Although

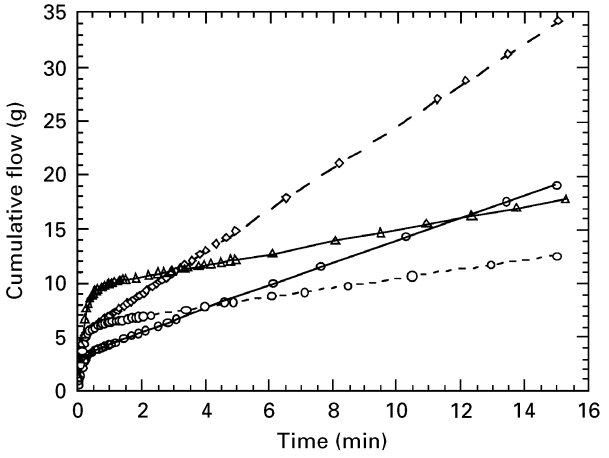

Figure 7 Effect of sizing type on flow response: (◇) 365 sized fibre; (△) 933 sized fibre; (○) dashed line – 449 sized fibres; (○) solid line – 463 sized fibres.

TABLE III Details related to flow experiments (resin: Dow Derakane 411-C50; fibre: S2 glass)

Sizing type	Number of tows	Volume fraction (%)	Pressure (psig)	Surface volume ratio $\times 10^5$ (m^{-1})
365	11	26	15	1.059
933, 449, 463	11	26	15	1.540

TABLE IV Flow rates in the two characteristic regimes as a function of sizing type

Fibre sizing type	Flow rate (g min^{-1})	
	Transient regime	Steady state regime
365	20.9	1.9
933	21.6	0.5
449	20.1	0.4
463	14.1	1.1

TABLE V Computed values of capillary pressure for the sized fibre–resin combinations

Fibre–resin pair	Capillary pressure $\Delta P_c \times 10^4$ (dyne cm^{-2})
S2-365/411-C50	76.6
S2-933/411-C50	78.1
S2-463/411-C50	97.8
S2-449/411-C50	99.6

permeabilities were not measured in these experiments it should be noted that in the initial state, local permeabilities, as measurable across each fractional area, could be different due to movement of fibres and degree of misalignment. In this case the true permeabilities should be determinable through the use of:

$$K = \frac{\Delta P r^2}{\varphi \eta L} \frac{1}{A} \sum \frac{\varepsilon_i^2}{(1-\varepsilon_i)^2} A_i \quad (7)$$

where ΔP is the pressure drop across length L, r is the fibre radius, φ is the rate of infusing flow, η is the viscosity of the infusing resin, A is the overall cross-sectional area (in this case of the tube), and ε_i is the porosity of each fractional area A_i [25]. From Fig. 7 it is clear that the transient period is most pronounced in the 933 system, whereas the order of values for the steady state flow rates (as also listed in Table II) is: $365 \gg 463 > 933 \sim 449$. It is interesting to note that the 365 system which is specifically sized for vinylesters and polyester shows the highest steady state flow rate, whereas the 933 system which is sized for higher temperature resin systems such as BMIs and PEEK show the longest transient flow period and one of the lowest flow rates, clearly indicating the effect of sizing type on infusion at the microlevel. One could visualize that flow through the fibre system occurs in steady state in a series of parallel streamlines formed by interconnected flow areas. Although the fibre volume fractions for the four systems under consideration are equal, the fibre surface area to volume ratio is significantly lower for the 365 sized system as a result of the larger diameter and this could be hypothesized to contribute at least partially to the effects summarized in Table IV. However, the other three systems differ only in sizing type and have the same diameter. It should be noted that even in these three systems there are significant differences between the flow rates, which does indicate an effect due to sizings. Experiments conducted on the same sized systems, but using an epoxy resin system also show similar trends, emphasizing the effect of sizings on microflow, which appears to contradict the previous results of Williams *et al.* [25] who postulated that under "steady state conditions no interface effects during cure can be expected".

Flow experiments conducted using clear tubes (in order to visualize the phenomena described earlier) demonstrate that the initial relatively rapid flow rate in the transient regime was a result of flow channelling around fibre bundles, which is a macroscopic phenomenon. Resin spreads from the initial channels and flow paths, eventually surrounding all the tows, due to radial flow initiated by capillary forces. Such capillary forces are directly affected by physical and chemical interactions between the fibre surface and the infusing resin. Assuming that the transverse spaces between individual fibres can be treated as cylindrical tubes, the capillary pressure, ΔP_c, associated with resin infusion within a fibre bundle, can be expressed as [26]:

$$\Delta P_c = \frac{2\gamma_l}{R} \cos\theta \quad (8)$$

where R represents the effective radius, γ_l the resin surface tension and θ the fibre–resin contact angle. Using the Young–DuPré equation to relate the contact angle, θ, to the resin surface tension, fibre surface tension, γ_s, and the interfacial tension, γ_{sl}, the capillary pressure can further be expressed as:

$$\Delta P_c = \frac{2}{R}(\gamma_s - \gamma_{sl}) \quad (9)$$

Using the relationship for surface tension suggested by Kaelble [7] to account for the polar and dispersive components of the interactions, the interfacial tension can be expressed as:

$$\gamma_{sl} \approx \gamma_s + \gamma_l - 2(\gamma_s^p - \gamma_l^p)^{1/2} - 2(\gamma_s^D - \gamma_l^D)^{1/2} \quad (10)$$

using which, the capillary pressure can be expressed as:

$$\Delta P_c \approx \frac{1}{R}[(\gamma_s^p - \gamma_l^p)^{1/2} + (\gamma_s^D - \gamma_l^D)^{1/2}] \frac{-2\gamma_l}{R} \quad (11)$$

It is expected that this expression should provide a reasonable estimate of the effect of fibre surface treatment on capillary flow, and hence on the transient flow regime itself.

Experimentally measured values of the polar and dispersive components of the surface free energies of the 4 differently sized S2 fibre types, as well as the surface tension measurements for the 411-C50 vinylester resin are reported in Table II. Capillary pressures for the fibre–resin combination computed using the equation for capillary pressures as determined from surface tension interactions are given in Table V assuming a 1 μm sized capillary radius. It could reasonably be expected that the duration of the transient region would be shorter for higher values of capillary pressure, and this is corroborated, albeit qualitatively, by a comparison between the experimental results (as in Fig. 6) and the predictions as given in Table V, with the exception of the 365 sized fibre, where again, physical dimensions could be responsible for the

observed differences. It should be noted that the ascending order of the capillary pressures ($449 > 463 > 933$) is the same as that shown by the duration of transient flow. Since the duration is a measure of the efficacy of wet-out, the results clearly indicate that fibre-sizing interactions do affect the rate of tow impregnation, and hence that of overall infusion and wet-out of a composite part.

4. Cure characterization

Resin transfer moulded parts can be cured under two generic regimes, (a) room temperature cure, wherein heat is generated purely due to the exothermic nature of chemical reactions, and (b) elevated temperature cure, wherein heat is supplied externally through the tool surface. The actual selection of one regime over another depends on a number of factors that include the type of resin system being used, application temperature of the product, rate and number of parts to be processed through the same tool etc., details of which may be found in Steenkamer *et al.* [27]. In most production processes, however, especially where a large number of parts have to be fabricated, and when uniformity and repeatability are critical, elevated temperature cure is the norm. Due to the low thermal conductivity of the preform reinforcement and the infusing vinylester resin, the centre of a given cross-section is at a lower temperature than the material close to the tool surface. Heat generated through the exotherm, further accelerates the chemical reactions between the resin and catalyst, resulting in completion of cure. Although this is a critical stage in the RTM process, it perhaps has received the least emphasis by investigators at a level further than that of global heat transfer under isothermal, or at best sequential isothermal (to model a non-isothermal process) conditions. However, it should be noted that extreme care is required during this stage, and in the selection of materials and process conditions that come into play during cure, if uniformity and good performance characteristics are required of the composite. Beyond the reactivity of the resin, and the reactivity and amount of catalyst, factors such as temperature, type and volume fraction of fibres, location of resin and fibre rich zones (such as near inserts and corners respectively), type and reactivity of sizing also need to be considered. This is an important differentiator, at least at the generic level, between the processing of thermoplastic and thermosetting composites, since the latter necessitates the inclusion of understanding of both rheology and polymerization reaction kinetics during the cure stage.

Although the problem of heat transfer associated with fluid flow through porous media has been investigated by a large number of researchers [28–30], there is a significant lack of accord on the feasibility and methodology of analysis. Of the two general categories, two phase models and equilibrium models, the equilibrium approach is considered more applicable to processes such as RTM. However, it is based on the assumption that the infusing resin and the preform have the same temperature at every point under consideration, which is analogous to assuming that the heat transfer coefficient is intrinsically infinite. This is obviously a gross assumption, since the value is finite and is required to be measured experimentally for each resin/fibre combination in the two phase approach. Despite this assumption, made because of the inability to theoretically predict the local heat transfer coefficient, an energy equation of the general form:

$$\phi\rho_r C_{\rho r}\left(\frac{\partial T}{\partial t} + u\frac{\partial T}{\partial x} + v\frac{\partial T}{\partial y}\right) + (1-\phi)\rho_f C_{\rho f}\frac{\partial T}{\partial t} = K\left(\frac{\partial^2 T}{\partial z^2}\right) + \phi S \tag{12}$$

can be used. Here, ϕ is the porosity of the perform, T is the temperature (with the assumption that the perform and resin both have the same temperature), t is the time, u and v are the gap wise averaged velocities in the x and y directions respectively, ρ_r and ρ_f are the densities of the resin and fibre respectively, $C_{\rho r}$ and $C_{\rho f}$ are the corresponding heat capacities. K is the combined conductivity and S is the energy generated in the resin during cure. This term (energy) is the most important, since it represents the actual cure kinetics of the composite through the formulation:

$$S = RE \tag{13}$$

where R is the rate of reaction and E is the heat of reaction. It should be noted that the specifics related to cure kinetics are intrinsically linked to factors such as the type of resin and fibres, sizing or surface treatment used, and the fibre volume fraction.

It is well known that the cure kinetics of anhydride- and amine-cured epoxy systems are affected by fibre surface treatments [1, 31–33], through potential reactions with acidic groups such as carboxylic acids and phenolic hydroxyls, and epoxide rings and amines, or through reactions of the aliphatic and non-acidic hydroxyls with epoxides and through reactions of quinone and carbonyl surface groups with amines. The effect of surface and sizing treatments on polyester cure kinetics has been elucidated in references [34–36], wherein it was shown that the addition of fibres to the resin caused changes in the overall rate of cure and final conversion. It should be noted that the actual mechanisms through which such changes are affected differ depending on the resin–reinforcement pair of interest. For example, the cure kinetics of addition polymerizations such as in amine-cured epoxies may be influenced by the preferential absorption of one resin component over the other onto the reinforcement surface, or by reactant dilution effects resulting from sizing dissolution. On the other hand, the cure kinetics of free radical chain polymerizations such as in polyesters and vinylesters may be affected by a variety of mechanisms, including surface deactivation of free radicals and diffusion effects. It was shown in the earlier section, that flow was affected not only by the presence of fibres, but also by the sizings on them. In similar fashion, cure mechanisms are affected at the microscale level through interactions with the sizings used.

4.1. Experimental procedure

Cure kinetics of the neat and fibre modified Dow-Derakane 411-C50 vinylester with 1.75 wt % Witco VSP-245 peroxide were investigated using a DuPont model 9900 Differential Scanning Calorimeter (DSC). Isothermal experiments were conducted at 90, 100, 110 and 120 °C for the neat and fibre-modified systems to measure heat evolution as a function of time. A minimum of three runs were performed per temperature and material pair. A nominal fibre loading of 20 vol % was used for the experiments using the 933, 365, 463 and 449 sized glass fibres. The samples were prepared by adding the proper amount of resin to a DSC sample pan containing a pre-weighed amount of chopped fibre (~4 mg). Care was taken to ensure that the sample pans were hermetically sealed in order to avoid styrene evolution during cure. Following isothermal cure, temperature scans from ambient temperature to 200 °C at a rate of 10 °C min^{-1} were conducted to measure residual heats of reaction.

The DSC provides the rate of heat evolution as a function of time, $q(t)$, for a sample of mass, m. The rate of change of polymerization, $d\alpha(t)/dt$, can hence be related to $q(t)$ through:

$$\frac{d\alpha(t)}{dt} = \frac{q(t)}{m\Delta H_r} \tag{14}$$

where ΔH_r is the specific heat of reaction. The total heat of reaction for a sample of mass m ($Q_{tot} = m\,\Delta H_r$) can be obtained from DSC measurements by summing the heat evolved during isothermal experiments, Q_i, with the residual heat, Q_r, obtained from subsequent temperature ramps:

$$Q_{tot} = Q_i + Q_r \tag{15}$$

For the present investigation, the heat of reaction for the 411-C50 vinylester was taken as the average value of multiple runs under reaction conditions which yielded the highest total heat, i.e., 425 ± 15 J g^{-1}. Simplified autocatalytic second-order kinetic equations have been successfully used previously to model the cure of styrene-based thermoset resins [37, 38]. Although empirical, a form of the equation:

$$\frac{d\alpha(t)}{dt} = k\alpha(t)^m[1 - \alpha(t)]^n \tag{16}$$

where $m + n = 2$ and k is the reaction rate constant, has been successfully used in the literature [37, 39, 40] to elucidate key aspects of polyester cure. The same second-order rate equation is employed herein to aid in the comparison of fibre–sizing effects on the cure kinetics of the vinylester system used.

4.2. Results and discussion

Fig. 8 shows thermograms obtained for neat vinylester at 90, 100, 110 and 120 °C for three sets of data each to demonstrate the repeatability of the DSC experiments. Fig. 9 shows thermograms obtained for the 365 sized S2 glass filled vinylester at 90, 100, 110 and 120 °C. These data are representative of experiments carried out with the other sizings as well. It should be noted

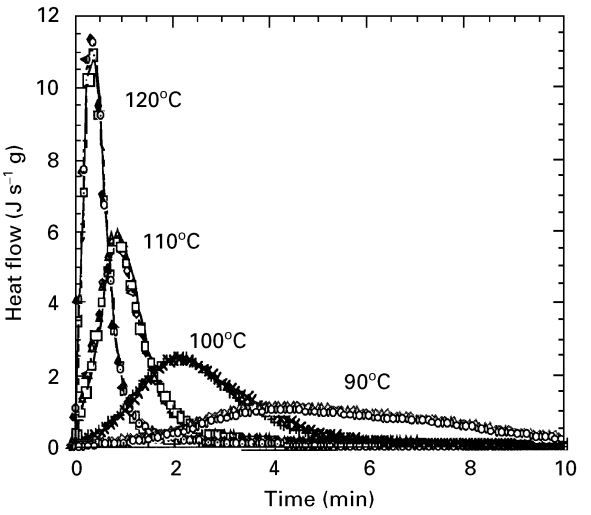

Figure 8 Thermograms for the unfilled vinylester system as a function of the isothermal temperature level.

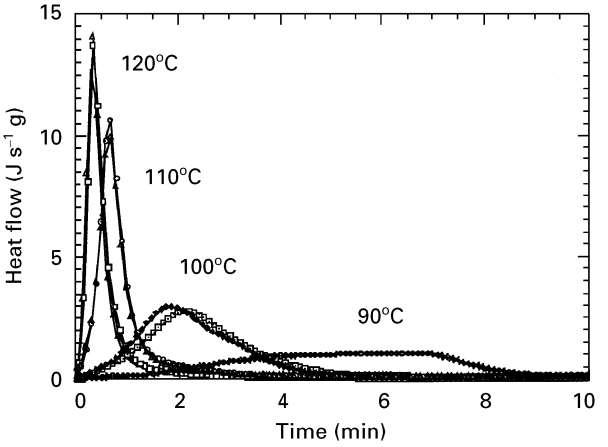

Figure 9 Thermograms for the vinylester system with the 365 sized glass fibres as a function of the isothermal temperature level.

that the repeatability suffers slightly in the presence of fibres, particularly at the lower temperatures. Although the reason for this is still unclear, it may be hypothesized that this is due to incomplete polymerization and the effect of secondary mechanisms that become dominant at the lower temperatures. In the case of both the unfilled (Fig. 8) and filled (Fig. 9) systems, a decrease in temperature results in a shift to the right, i.e., a longer time period to peak, as well as a decrease in the total heat flow resulting from the reaction. It can also be seen that the presence of fibres results in a faster attainment of peak heat flow and a higher peak heat flow value. A better comparison of the effects of sizing through the use of differently sized systems can be made through a comparison of the autocatalytic rate parameters, k and m. Average values of k and m ($n = 2 - m$) obtained by fitting DSC data to the second-order autocatalytic equation for neat and sized fibre filled 411-C50 vinylester are given in Table VI. It can be noticed that the values of k increase with the addition of the sized fibres, whereas those of m decrease. A study of the correlation coefficients obtained for the values of k and m show that with the exception of the filled systems at 90 °C, the data are

TABLE VI Average rate constants using the autocatalytic rate expression: $d\alpha(t)/dt = k\alpha(t)^m[1 - \alpha(t)]^n$, where $m + n = 2$

System	Temperature (°C)	k (1 min^{-1})	m
Neat resin	90	0.711	0.772
	100	1.316	0.717
	110	2.630	0.617
	120	5.050	0.528
365 sized S2 gass	90	–	–
	100	1.494	0.721
	110	3.770	0.540
	120	5.250	0.414
365 sized S2 glass stripped	90	–	–
	100	2.750	0.602
	110	4.670	0.430
	120	9.940	0.585
449 sized S2 glass	90	0.709	0.920
	100	1.617	0.733
	110	3.580	0.416
	120	5.310	0.472
463 sized S2 glass	90	–	–
	100	1.810	0.701
	110	3.630	0.577
	120	5.410	0.512
933 sized S2 glass	90	–	–
	100	1.400	0.721
	110	3.410	0.583
	120	5.570	0.449

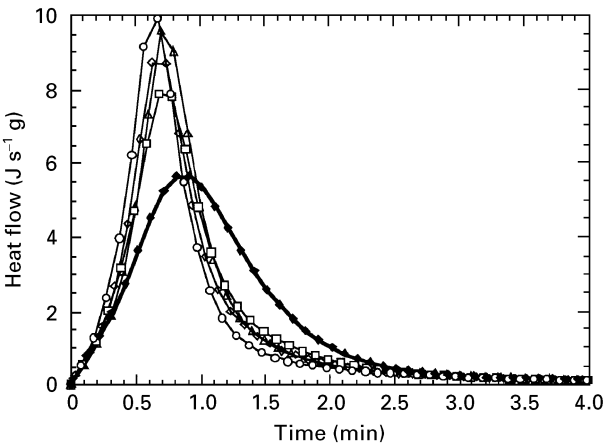

Figure 10 Isothermal cure thermograms for; (◆) unfilled Dow Derakane 411-C50; (△) Owens-Corning 449 sized; (◇) 463 sized; (□) 933 sized and (○) 365 sized S2 glass filled vinylester at 110 °C.

generally amenable to analysis using the form of the autocatalytic reaction described earlier. From the results in Table VI, it is clear that the presence of the different sizings affects the reaction rate significantly, and this is emphasized through a comparison of the results obtained using the 365 sized system and the fibre system obtained by stripping the 365 sizing off through the use of acetone.

Fig. 10 depicts DSC thermograms comparing the reaction rate of neat vinylester to that of filled systems containing the 449, 463, 933 and 365 sized S2 glass fibres at 110 °C. It is apparent that in all cases the filled systems cure significantly more rapidly than their neat unfilled resin counterpart. It is significant that

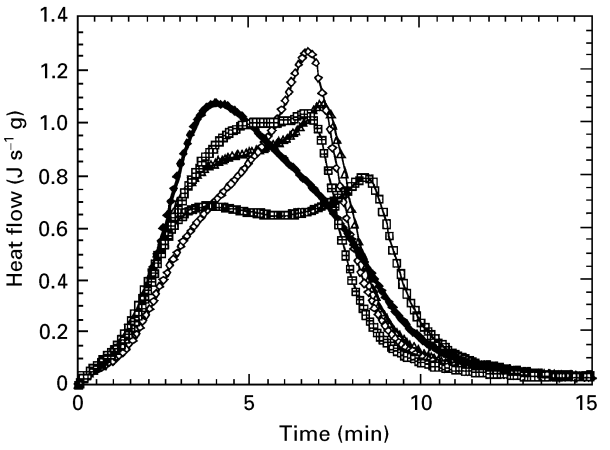

Figure 11 Isothermal cure thermograms for; (◆) unfilled Dow Derakane 411-C50; (△) Owens-Corning 449 sized; (◇) 463 sized; (□) 933 sized and (■) 365 sized S2 glass filled vinylester at 90 °C.

the peak heat flow for the filled systems is achieved 30–40% faster than the neat system. Although more pronounced at 110 °C, the same effect is noticed at 100 and 120 °C. However, Fig. 11 indicates that at 90 °C the fibres tend to affect cure behaviour by retarding polymerization. The data in the latter thermograms, with the exception of those for neat vinylester, are clearly not amenable to analysis by the simple rate equation used herein. It is worthwhile noting that the thermogram depicting cure of the 933 sized system shows the maximum deviation from expected behaviour. This system, as was described earlier showed more fully condensed silane and a lack of unbound epoxy when characterized using the FTIR, which could be a partial explanation for the observed behaviour. Silane coupling agents are known to participate in the cure kinetics of vinylester resin when suitably initiated by temperature, whereas the untreated glass surface could actually inhibit polymerization. A combination of effects including that of insufficient heat and lack of suitable linkages/active sites can be suggested as the reason for the behaviour at 90 °C. Obviously further research is warranted into such phenomena, especially since there would appear to be a move in industry towards RTM derivatives such as resin infusion and Seemann Composites Resin Infusion Molding Process (SCRIMP), where cure is conducted at room or at lower elevated temperature regimes, such as would be represented by the 90 °C temperature.

Reactivities over wider temperature ranges can be easily compared through the use of Arrhenius plots for the determination of levels of activation energy and pre-exponential factors. Fig. 12 shows the comparison between the Arrhenius plots for the neat and the 365 sized-filled systems. While the linear relationship between the reciprocal of temperature and the logarithm of the rate constant is clear for the neat resin, the 365 sized-filled system, which is characteristic of the other filled systems investigated herein, exhibits a marked non-linear response, which may be an indication of competing cure processes. Table VII reports values of activation energy (E_a), and pre-exponential factors, A, obtained by the Arrhenius analysis of data between

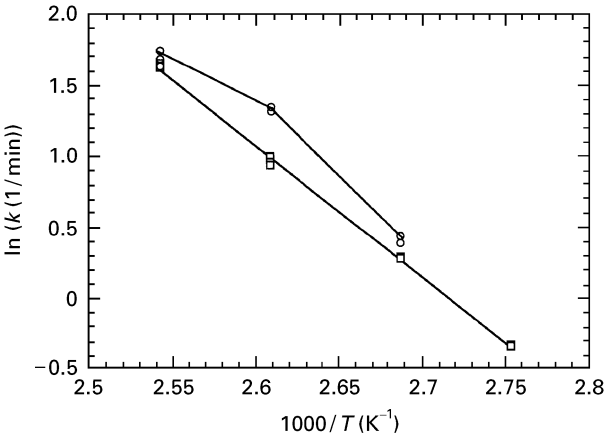

Figure 12 Arrhenius plots for; (□) unfilled Dow Derakane 411-C50, and (○) Owens-Corning 365 sized S2 glass filled vinylester systems.

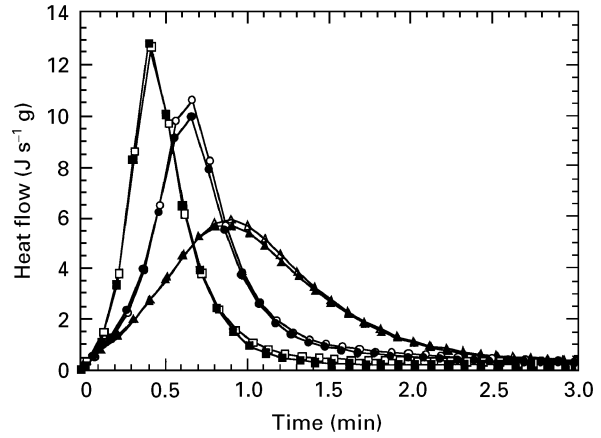

Figure 13 Isothermal cure thermograms for; (△) unfilled Dow Derakane 411-C50; (○) Owens-Corning 365 sized and (□) stripped 365 sized S2 glass filled vinylester at 110 °C.

100 and 120 °C for the filled systems and between 90 and 120 °C for neat vinylester. Activation energies for the 449, 463 and stripped 365 system are substantially lower than the levels for the neat 411-C50. In the case of the stripped system, 365 sized fibres were washed in acetone in an attempt to remove the sizing. The 365 fibres treated in this manner significantly reduced the apparent activation energy for cure. The increased cure rate resulting from stripping is shown by thermograms in Fig. 13. This analysis suggests that the presence of sized fibres decreases the apparent activation energy which is in agreement with the observed accelerated cure rates. Three major points can be drawn from the results presented above. First, at cure temperatures in the range of 100–120 °C, the presence of S2 glass fibres substantially increases the cure rate of the Dow Derakane 411-C50 vinylester. Second, the type of fibre sizing or surface treatment can significantly affect the degree of cure acceleration. Finally, at lower temperatures (90 °C in this case) the enhancing effect is diminished and in some cases replaced by a retarding effect (Fig. 11).

Several investigators have noted increased and decreased reaction rates for filled polyester systems. Lee and Han [35] investigated the effects of silane-treated and untreated glass beads (fillers) on the cure of polyester systems. They found that bare glass beads reduced the reactivity of the polyester system, while a silane coating produced a lesser decrease. Ishida and Koenig [34] found that bare E-glass fibres retarded cure of polyester systems. This was attributed to a decrease in free radical concentration resulting from the formation of charge transfer complexes between the free radicals and the inorganic oxides. Assuming that the basic mechanisms of cure are common to the polyester and vinylester systems, such surface terminations cannot account for the accelerated cure behaviour observed in the current investigation. Lem and Han [36] investigated the effects of inorganic fillers on the cure behaviour of polyester systems and found that calcium carbonate in particular accelerated polyester cure. This was attributed to an apparent enhancement of the rate of peroxide decomposition on the effects of fillers and reinforcements on the cure kinetics of free radical chain polymerization. These mechanisms are intrinsically not well understood, although fillers are routinely used in processes such as pultrusion to increase conductivity and hence cure within the die. With this in mind, a brief discussion regarding free radical chain polymerization, as applicable to fibre–resin surface based interaction proves helpful in understanding possible accelerative and retarding mechanisms, such as those seen in the present investigation.

4.3. Radical chain polymerization

The vinylester cure process is a free radical chain polymerization process which can be broken into three stages: (a) the inhibition stage, (b) the propagation stage, and (c) the diffusion-limited stage. During the inhibition stage, radicals, which are generated by the decomposition of the initiator, are consumed by the inhibitors. Once the inhibitors are consumed, the polymerization rate increases throughout the propagation stage. Finally, the diffusion-limited regime is reached when increases in molecular weight limit the mobility of the reacting species and hinder propagation. The kinetics of free-radical polymerization (particularly linear polymerization) have been studied extensively [41]. Several phenomena that influence the rates of chain polymerization may provide clues to the mechanisms by which sized S2 glass fibres accelerate the cure of vinylester. The following is a discussion of such phenomena and their possible relation to the effect of fibre sizing on cure.

4.3.1. Inhibitors

Radical-chain polymerization is suppressed by the presence of inhibitors and retarders. These substances act by reacting with initiating and propagating free radicals and converting them to species that will not sustain propagation or that possess substantially lower reactivity [41]. Inhibitors are commonly used by resin manufacturers to prolong resin shelf life and to broaden processing windows. Quinones such as *p*-benzoquinone and chloranil (2,3,5,6-tetrachlorobenzoquinone) are an important class of inhibitors whose

behavior is complex. In general, they react to form low-reactivity radicals. Furthermore, the quinones commonly used are electron poor in nature and provide a strong inhibition for electron-rich materials such as styrene. Depending on surface characteristics inhibitors such as quinones interact strongly with the surfaces of reinforcements. Hence, absorption of the inhibitors onto the surfaces of the fibres could result in apparent increases in the rates of polymerization. On the other hand, it should be noted that fibre surfaces may themselves act as inhibitors, scavenging free radicals and reducing polymerization rates. Yet, one may postulate that under appropriate conditions, inhibitor absorption may outweigh surface scavenging effects and yield an overall increase of the polymerization rate. The driving force for inhibitor absorption will be related to its interaction with the surface. Hence, the surface energy characteristics of the reinforcement/sizings should significantly affect cure behaviour provided this mechanism is in play.

4.3.2. Diffusion effects

Typically, free-radical polymerizations exhibit an acceleration in the rate of polymerization such as that exhibited by the vinylester system being investigated. This behaviour is a result of hindered translational mobility of the reacting species. As a result of such diffusion limitations, bimolecular termination is hindered and the resulting increase in free radical concentration accelerates the reaction. This effect is known as the "Trommsdorff," or "gel," effect [42]. The presence of fibres may physically reduce molecular mobility and thus enhance such an effect. On the other hand, using a similar argument, reduced mobility resulting from the presence of fibre surfaces can aid radical trapping (unimolecular termination) and decrease initiator efficiency [43], which might suppress polymerization rates.

4.3.3. "Matrix" polymerization

The addition of stereoregular polymers to monomers has been found to accelerate polymerization rates [44]. In general, the growing radical associates with the added polymer, and propagation occurs with the radical bound to the "matrix". As a result, segmental mobility of the growing chain is reduced, and the termination rate is decreased. It is possible that reacting radicals associate with the fibre surfaces, reducing the segmental mobility necessary for termination and increasing the observed polymerization rate.

4.3.4. Effects of fibre surface energy

Of the mechanisms decribed briefly above, the absorption of inhibitors will be particularly affected by the fibre-surface free energy levels, since these depend on the chemical composition of the fibre surface and will affect fibre–inhibitor interaction energies. It may be recalled from Table II, that the polar components of the surface free energy for the fibre–sizing combinations under consideration were significantly lower than the dispersive component. It is also interesting to compare the surface free energy components of the stripped 365 system where $\gamma^{p} = 3.39 \pm 1.43$ dyne cm^{-1} and $\gamma^{D} = 35.48 \pm 3.85$ dyne cm^{-1} with the corresponding values for the unstripped system reported in Table II ($\gamma^{p} = 8.60 \pm 1.18$ dyne cm^{-1} and $\gamma^{D} = 33.09 \pm 1.92$ dyne cm^{-1}). Not only does the stripped system have a lower overall surface free energy level, but the polar contribution is extremely low. This is probably due to the removal of the relatively more polar epoxy during stripping. It is clear that surface free energy could play a significant role in determining the degree of cure rate enhancement for glass filled vinylester systems and in fact a strong relationship does exist between the polar surface free energy and the degree of vinylester cure activation. Fig. 14 shows activation energies for the fibre modified vinylester cure (reported in Table VII) plotted as a function of the polar component of the fibre surface free energies. It can be seen, that in general, a lower polar surface energy comports a decrease in activation energy and a more pronounced acceleration of the vinylester cure. It is expected that electron-poor inhibitors might exhibit a greater affinity for electron-rich surfaces. This suggests that the less polar surfaces might absorb a larger amount of inhibitor than the more polar surfaces, thus increasing reaction rates, as observed in this investigation.

It is clear that the cause for the observed fibre accelerated cure must be closely linked to interactions between resin components and the surface composition of the fibre/sizing system. Differences in fibre surface energy are not expected to influence diffusivity,

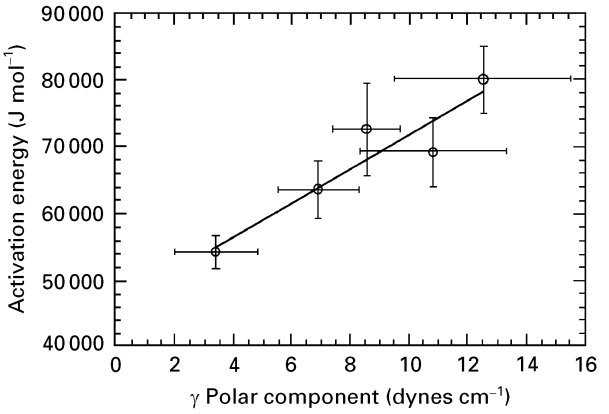

Figure 14 Activation energies for the S2 glass fibre filled Dow Derakane 411-C50 vinylester resin system plotted as a function of the polar components of the fibre surface free energies.

TABLE VII Arrhenius parameters

Material type	E_a (J mole^{-1})	I_n (A) (1 min^{-1})
Neat 411-C50 vinylester	77 407 ± 1000	25.29 ± 0.32
365 sized S2 glass	72 482 ± 6957	23.91 ± 2.18
Stripped 365 sized S2 glass	54 146 ± 2320	25.31 ± 0.65
449 sized S2 glass	69 058 ± 5252	22.87 ± 1.65
463 sized S2 glass	63 447 ± 4409	21.14 ± 1.39
933 sized S2 glass	79 828 ± 4981	26.19 ± 1.57

and it is not foreseeable that the mechanism of "matrix" polymerization is affecting vinylester cure. It would therefore appear that surface absorption of inhibitors is a plausible explanation for the fibre-induced cure acceleration.

5. Summary

In this work the effect of commercially available S2 glass sized fibre systems on micro-infusion and subsequent cure of vinylesters was investigated. It was found that coupling agent–resin interactions have a significant effect on these phenomena, leading to the definite establishment of the importance of understanding mechanisms both at a macro- and a microscopic level. It was found that the surface free energies of the different sized fibres are significantly varied, and that the resulting differences in fibre–resin compatibility at the boundary layer influences flow behaviour. In particular a significant retardation in the flow of resin into fibre bundles is noticed for fibre–resin systems expected to possess lower capillary driving forces. Sizing–resin compatibility thus not only plays a significant role in ensuring complete wet-out of infused surfaces, but also controls the rate at which wet-out occurs. The dwell time needed for wet-out could then be construed as a hitherto unknown controlling factor in the speed at which the RTM process can be completed. Care must be taken to ensure that for a given sizing–resin combination, adequate time is allowed for complete tow/bundle infusion and wet-out, else a poorly filled and bonded composite will ensue. The same sizings are seen to have a significant effect on cure kinetics, with some results suggesting that the absorption of inhibitors from the infusing resin system onto fibre surfaces is responsible for the drastic changes in cure behaviour of the resin system in the presence of sized fibres. In fact, a relationship between the polar component of the fibre surface-free energy and the level of cure enhancement is proposed.

From the present study, it can be concluded that for true control of the RTM process (and like processes), a better understanding of phenomena at the microscopic-level is critical. Factors such as sizing reactivity and fibre volume fraction, which were taken for granted at the global or macroscopic-level, are in fact critical not only to final composite performance, but also during processing itself. The factors, which intrinsically are involved at the level of the interphase provide a cogent and strong link between the three interrelated aspects of materials, processing performance (as further elucidated by Karbhari and Palmese [45]). It is emphasized that the true development of an understanding of mechanisms at this scale will lead to the development of a viable (and less empirical) processing since base for composites in general and one that will enable true tailoring of materials for optimized processing and performance.

Acknowledgements

The authors wish to thank Timothy L. Collins of Owens-Corning for supplying the sized S-2 glass rovings. Helpful discussions with Professor Roy L. McCullough are also gratefully acknowledged. The assistance of Ole A. Andersen, Danny Gan and Morris Deputy in conducting some of the experiments is also acknowledged. The first author would also like to acknowledge the University of California, San Diego which enabled the completion of this work through start-up funds provided to him.

References

1. G. R. PALMESE and R. L. McCULLOUGH, *J. Adhesion* **44** (1994) 29.
2. T. P. SKOURLIS and R. L. McCULLOUGH, *Compos. Sci. Technol.* **49** (1993) 363.
3. D. L. LEYDEN and J. B. ATWATER, in "Silanes and other coupling agents", edited by K. L. Mittal (VSP, Utrecht, 1992) p. 143.
4. J. M. PARK and R. V. SUBRAMANIAN, *ibid.* p. 473.
5. F. J. BOERIO, C. A. GOSSELIN, R. G. DILLINGHAM and H. W. LIU, *J. Adhesion* **13** (1981) 159.
6. B. MILLER, in "Surface characteristics of fibres and textiles", Part II, edited by M. J. Schick (Marcel Dekker, New York, 1972).
7. D. H. KAEBLE, *J. Adhesion* **2** (1970) 66.
8. K. L. ADAMS and L. REBENFELD, *Textile Res. J.* (1987) 647.
9. *Idem*, *Polym. Compos.* **12** (1991) 179.
10. *Idem*, *ibid.* **12** (1991) 186.
11. R. DAVÉ and S. HOULE, in Proceedings of the 5th Technical Conference of the American Society for Composites (Technomic Press, Lancaster, PA, 1990) pp. 539–547.
12. V. M. KARBHARI, D. A. STEENKAMER and G. R. PALMESE, Society of Automotive Engineering Technical Paper 930166 (1993).
13. D. A. STEENKAMER, S. H. McKNIGHT, D. J. WILKINS and V. M. KARBHARI, *J. Mater. Sci.* **30** (1995) 3207.
14. J. KOZENG, "Sitzungsberichte wiener akademie der wissenshaft", Abt. IIa (1927) p. 136.
15. P. C. CARMAN (1937) *Trans. Inst. Chem. Eng.* (1937) 150.
16. R. B. BIRD, W. E. STEWART and E. N. LIGHTFOOT, "Transport phenomena" (Wiley, New York, 1960).
17. A. E. SCHEIDEGGER, "Physics of flow through porous media" (University of Toronto Press, Toronto, 1974).
18. A. S. SANGANI and A. ACRIVOS, *Int. J. Multiphase Flow* **8** (1982) 343.
19. J. E. DRUMMOND and M. I. TAHIR, *ibid.* **10** (1984) 515.
20. M. V. BRUSCHKE, PhD thesis, University of Delaware (1992).
21. G. W. JACKSON and D. F. JAMES, *Can. J. Chem. Engng.* **64** (1986) 364.
22. F. R. PHELAN, in Proceedings of the 7th Technical Conference on Composite Materials (Technomic Press, Lancaster, PA, 1992).
23. R. S. PARNAS and F. R. PHELAN, *SAMPE Quarterly* **22** (1991) 53.
24. G. R. PALMESE and V. M. KARBHARI, *Polym. Compos.* **16** (1995) 313.
25. J. G. WILLIAMS, C. E. M. MORRIS and B. C. ENNIS, *Polym. Engng. Sci.* **14** (1974) 413.
26. J. N. ISRAELACHVILI, "Intermolecular and surface forces" (Academic Press, New York, 1985) pp. 213–220.
27. A. STEENKAMER, D. J. WILKINS and V. M. KARBHARI, *Processing of Advanced Mater.* **3** (1993) 181.
28. V. N. GONZÁLEZ and C. W. MACOSKO, in Proceedings of the 2nd International Conference of Reactive Processing of Polymers, edited by J. T. Lindt (University of Pittsburgh, Pittsburgh, PA) (1982).
29. C. L. TIEN, *Adv. Appl. Mech.* **27** (1990) 225.
30. M. UENOYAMA and S. I. GÜÇERI, Analysis and simulation of structural reaction injection molding, Center for Composite Materials Report CCM-91-09 (1991).

31. A. GARTON and W. T. K. STEVENSON, *J. Polym. Sci. Part A: Polym. Chem.* **26** (1988) 541.
32. J. MIJOVIC and H. T. WANG, *J. Appl. Polym. Sci.* **37** (1989) 2661.
33. A. GARTON, W. T. K. STEVENSON and S. P. WANG, *J. Polym. Sci. Part A: Polym. Chem.* **26** (1988) 1377.
34. H. ISHIDA and J. L. KOENIG, *J. Polym. Sci. Polym. Phys. Ed.* **17** (1979) 615.
35. D.-S. LEE and C. D. HAN, *J. Appl. Polym. Sci.* **33** (1987) 419.
36. K.-W. LEM and C. D. HAN, *ibid.* **28** (1983) 3185.
37. C. D. HAN and K.-W. LEM, *ibid.* **28** (1983) 3155.
38. P. W. K. LAM, H. P. PLAUMANN and T. TRAN, *ibid.* **41** (1990) 3043.
39. M. R. KAMAL and S. SOUROUR, *Polym. Engng. Sci.* **13** (1973) 59.
40. P. W. K. LAM, *Polym. Compos.* **8** (1987) 427.
41. G. ODIAN, "Principles of polymerization" (John Wiley, New York, 1981) p. 179.
42. T. J. TULIG and M. T. TIRRELL, *Macromolecules* **14** (1981) 1501.
43. G. L. BATCH and C. W. MACOSKO, *J. Appl. Polym. Sci.* **44** (1992) 1711.
44. J. GONS, W. O. SLAGTER and G. CHALLA, *J. Polym. Sci.: Polym. Chem. Edn.* **15** (1977) 771.
45. V. M. KARBHARI and G. R. PALMESE, in Proceedings of the 27th International SAMPE Technical Conference, Albuquerque, NM (1995) pp. 1035–1047.

Received 5 March 1996
and accepted 11 February 1997